



Compact multimode-resonator multiplexer with wide upper-stopband and high isolation

cambridge.org/mrf

Kaijun Song¹, Mou Luo¹ , Cuilin Zhong², Yuxuan Chen¹, Yedi Zhou¹
and Fei Xia¹ 

¹HF Key Laboratory of Science, University of Electronic Science and Technology of China, Chengdu 611731, China and ²Shen Zhen City Jiang Bo Chuang Xing Electronic Co. Ltd., Shen Zhen 518000, China

Research Paper

Cite this article: Song K, Luo M, Zhong C, Chen Y, Zhou Y, Xia F (2021). Compact multimode-resonator multiplexer with wide upper-stopband and high isolation. *International Journal of Microwave and Wireless Technologies* **13**, 111–118. <https://doi.org/10.1017/S1759078720001063>

Received: 27 December 2019
Revised: 15 July 2020
Accepted: 16 July 2020
First published online: 30 September 2020

Key words:

High isolation; miniaturization; multimode resonator; quadplexer

Author for correspondence:

Cuilin Zhong,
E-mail: zhzhongcuilin@126.com

Abstract

A miniaturized high-isolation quadplexer with wide upper-stopband based on open and short stub-loaded multimode-resonator is proposed in this paper. Based on the theory of multimode-resonator and stepped impedance resonator (SIR), the compact quadplexer is designed by using multimode-resonator and SIR. In order to further miniaturize the size of the circuit, the multimode resonator is employed as the common resonator to replace the common matching network of the quadplexer and the SIRs are curved. Equivalent topology circuit is given to analyze and design the quadplexer. Detailed analyses are given according to the equivalent circuits. The proposed compact quadplexer working at central frequencies of 1.8, 2.4, 2.8, and 3.5 GHz with over 40 dB isolation is finally simulated, fabricated, and measured. The measured results agree well with the simulated ones. The total size of the fabricated quadplexer is $0.36 \lambda_g \times 0.42 \lambda_g$.

Introduction

With the development of the wireless communication systems, the demand for various high-performance passive or active circuits has increased greatly [1–27]. In multiband communication systems, the multiplexer is an important and essential component in the RF front-end circuits. The multiplexer is used to transfer signals of different frequency bands to different channels, which is conventionally constituted from several bandpass filters and a multi-port matching network [1–7]. Microstrip planar multiplexers have been widely studied in recent years, due to the advantages of compact size, convenient integration, and ease in fabrication [8–15].

Traditional multiplexer adopts the structure of the cascade of multiple passbands by matching networks. However, with the increment in the number of the matching networks, not only the size of the circuit is large, but also it is difficult to optimize the circuit, which is mainly caused by the interaction between various filters [16–20]. So the design of common part in the form of common resonator is introduced in order to miniaturize the multiplexer circuit, which cannot contain external combining circuits [21–27].

In this paper, a quadplexer with compact size, wide upper-stopband, and high isolation is proposed. In order to reduce the size of the multiplexer, a multimode resonator with stub-loaded structure is used as the common resonator and the matching network is replaced. The resonant frequencies of multimode resonator can be adjusted by changing the lengths of the open stub and short stub, respectively, which is very flexible. Meanwhile, the coupling feed technology is used so that the multiplexer can be compact with the increment in the number of the channels. In addition, the presented miniaturized high-isolation quadplexer is designed and fabricated. Finally, the measured results agree with the simulated ones closely, which reveals that the proposed quadplexer has the advantages of wide upper-stopband, low insertion loss, good return loss, and high isolation. The total size of the fabricated quadplexer is $0.36 \lambda_g \times 0.42 \lambda_g$.

Analysis and design of the quadplexer

The structure of the presented miniaturized high-isolation quadplexer has been shown in Fig. 1. It consists of a common multimode resonator and four channels using stepped impedance resonators (SIRs). The multimode resonator with an open-circuit branch and a short-circuit branch is adopted as a common resonator to replace matching network, which is good for miniaturization. The four bandpass filters using the structures of SIRs are coupled with the common multimode resonator and the SIRs are curved in order to get compact circuit size. It can be seen from Fig. 1 that the two passbands (port 2 and port 5) at the bottom of the circuit are realized by a short-stub loaded quarter-wavelength SIR and an open-stub loaded half-wavelength split-ring SIR, respectively. The other two passbands (port 3 and port 4)

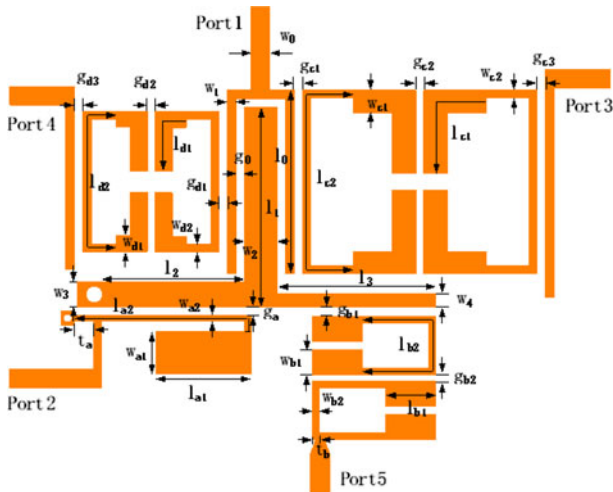


Fig. 1. Structure of the proposed quadplexer.

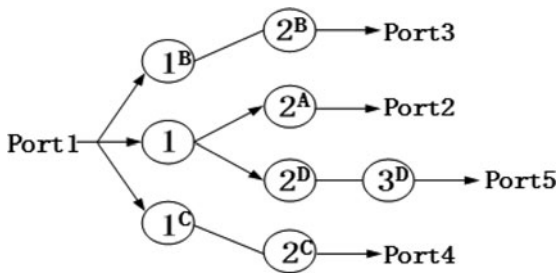


Fig. 2. The circuit topology of the quadplexer.

are realized by open-loop SIRs, which are coupling fed at the input feeder. The use of common resonator and the curved SIRs can further reduce the size of the circuit, making the overall circuit very compact.

Figure 2 illustrates the circuit topology of the quadplexer. The circle represents the resonator, and the solid line represents the coupling path between the resonators. The multimode resonator is coupled with the resonators of the four channels, respectively. It is obvious that the use of multimode resonator as the common resonator not only eliminates redundant resonators, but also eliminates additional matching circuits, which is helpful to achieve the miniaturization of the circuit.

The design procedure of the presented quadplexer can be summarized as three steps. Firstly, the common multimode resonator with an open-circuit branch and a short-circuit branch for desired operating frequencies is obtained by adjusting the lengths of the branches. Secondly, the two channels (port 2 and port 5) coupled with the short-circuit and open-circuit branches are realized by SIRs, and the central frequencies and relative bandwidths are 1.8/3.5 GHz and 5.1/5.7%, respectively. Finally, the other two channels (port 3 and port 4) are added at the input feeder by the coupling feed technology, and the central frequencies and relative bandwidths are 2.4/2.8 GHz and 2.6/2.5%, respectively. Figure 3 shows the structure of the stub-loaded multimode resonator, which is composed of an open-circuit stub and a short-circuit stub. The characteristic impedances are Z_1, Z_2, Z_3 , and the electrical lengths are $\theta_1, \theta_2,$

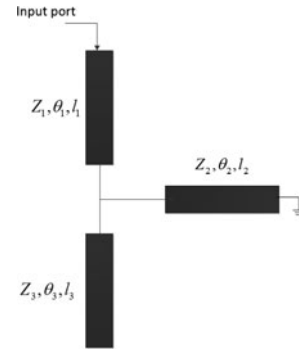
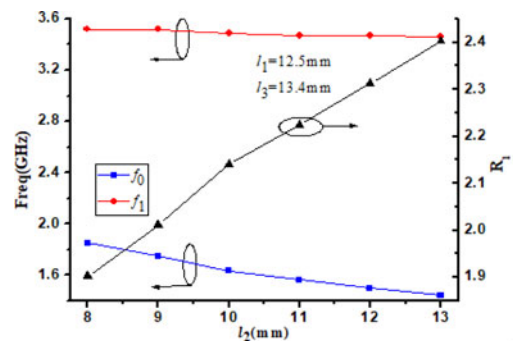
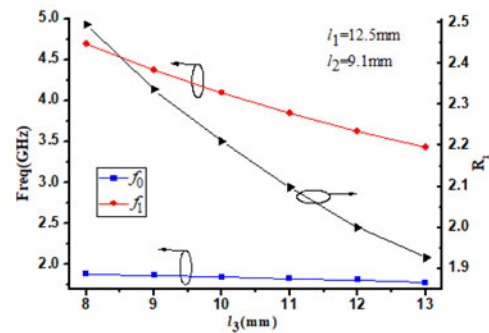


Fig. 3. The structure of the stub-loaded multimode resonator.



(a)



(b)

Fig. 4. The relationship between resonant frequencies and lengths of loaded stubs. (a) Frequency f_0 and f_1 with the length of l_2 . (b) Frequency f_0 and f_1 with the length of l_3 .

θ_3 , respectively, as shown in Fig. 3. The input impedance of the resonator can be achieved:

$$Y_{in} = \frac{\tan \theta_1 - T_1 \cot \theta_2 + T_2 \tan \theta_3}{Z_1(T_1 \cot \theta_2 \tan \theta_1 - T_2 \cot \theta_3 \tan \theta_1)} \quad (1)$$

When $Y_{in} = 0$, the resonant condition can be achieved:

$$\tan(\theta_1 \times R_n) - T_1 \cot(\theta_2 \times R_n) + T_2 \tan(\theta_3 \times R_n) = 0, \quad (2)$$

where $T_1 = Z_1/Z_2, T_2 = Z_1/Z_3$, and R_n is the ratio of n th harmonic frequency f_n to fundamental frequency f_0 . Then, the fundamental frequency f_0 and the first harmonic frequency f_1 of the dual-mode

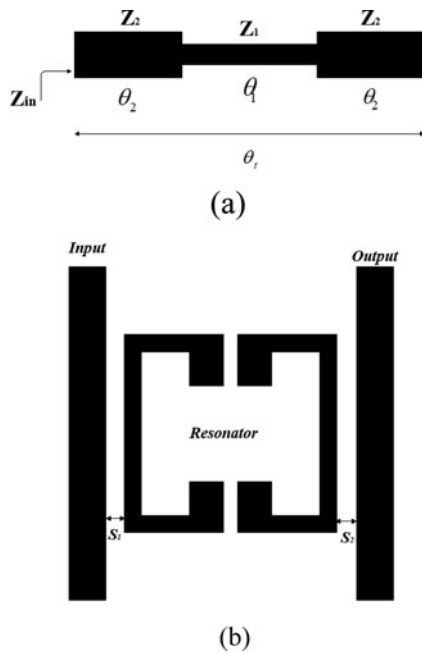


Fig. 5. The structures of stepped-impedance resonator and the coupling feed topology. (a) Stepped-impedance resonator. (b) Coupling feed topology.

Table 1. External quality factors and coupling coefficients

Channel	Central frequency (GHz)	Relative bandwidth (%)	Q_e	K
1	1.8	5.1	22.48	0.041
2	3.5	5.7	18.10	0.052
3	2.4	2.6	44.11	0.021
4	2.8	2.5	45.87	0.020

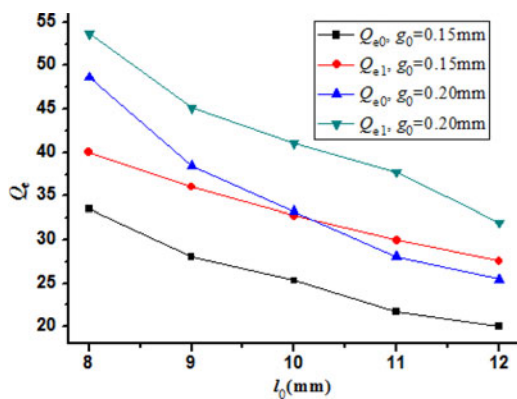
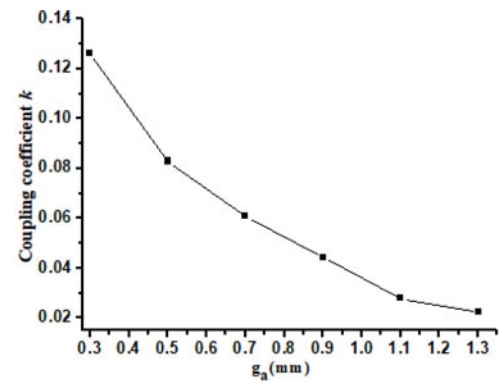


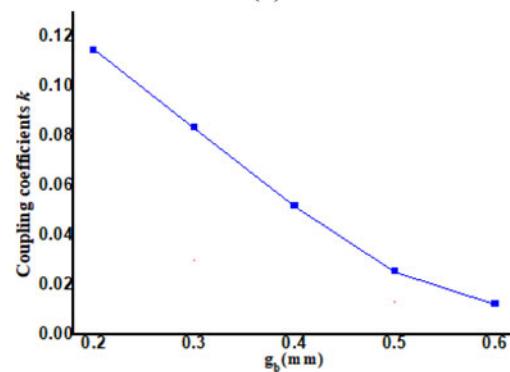
Fig. 6. Relationship between Q_e , l_0 , and g_0 .

resonator can be adjusted by changing the lengths of the short-circuit stub l_2 and open-circuit stub l_3 , respectively. In addition, the resonant frequencies of the short-circuit branch and open-circuit branch are 1.8 and 3.5 GHz, respectively.

The relationship between resonant frequencies and lengths of loaded stubs is given by Fig. 4 (where $T_1 = Z_1/Z_2 = 32/41 = 0.78$, $T_2 = Z_1/Z_3 = 32/84 = 0.38$, $l_1 = 12.5$ mm). It is obvious that the frequency f_0 can be adjusted by changing the length of shorted



(a)



(b)

Fig. 7. Coupling coefficient K . (a) Coupling coefficient between shorted SIR and common resonator. (b) Coupling coefficient between open-loop SIR and common resonator.

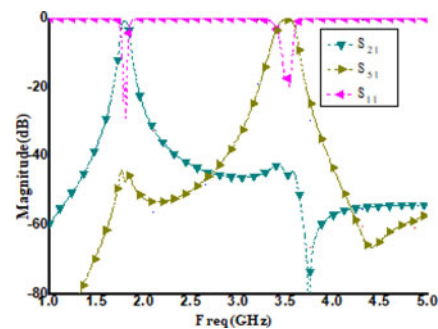


Fig. 8. Transmission response of channel 1 and channel 2.

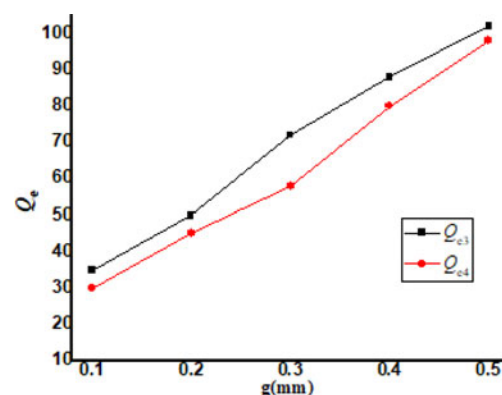


Fig. 9. External quality factors of the expanded channels.

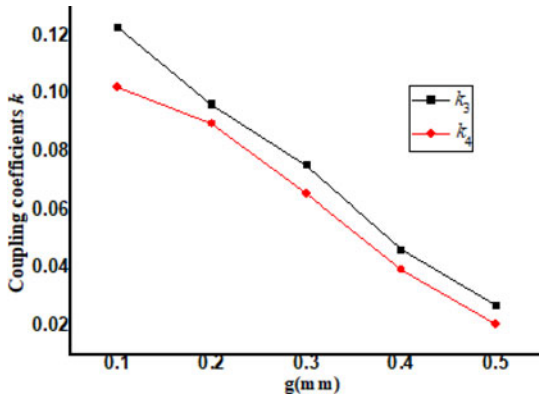


Fig. 10. Coupling coefficients of the expanded channels.

branch l_2 and there is almost no effect on f_1 . The frequency f_0 will be smaller with the increase of l_2 . In addition, the frequency f_1 can be adjusted by changing the length of open stub l_3 without any influence on f_0 , and f_1 will be smaller with the increase of l_3 . Thus, it is flexible to get desired operating frequencies by adjusting the lengths of the short-circuit stub l_2 and open-circuit stub l_3 , respectively. In the proposed circuit, the resonant frequencies of the short-circuit branch and open-circuit branch are 1.8 and 3.5 GHz, respectively. It is also easy to achieve the desired return losses at the different channels by changing the widths of the short-circuit stub and open-circuit stub separately, because the width of the microstrip is related to the characteristic impedance of the microstrip.

Figure 5 gives the structures of a stepped-impedance resonator and the coupling feed topology, and the SIR is curved in the proposed quadplexer to miniaturize the circuit. As illustrated in Fig. 5 (a), Z_1 and Z_2 are the characteristic impedances of the high-impedance and low-impedance line, respectively, and θ_1 and θ_2 are the electrical lengths of the high-impedance and low-impedance line, respectively. The total electrical length of the SIR is θ_t . The input impedance Z_{in} of the SIR is derived as

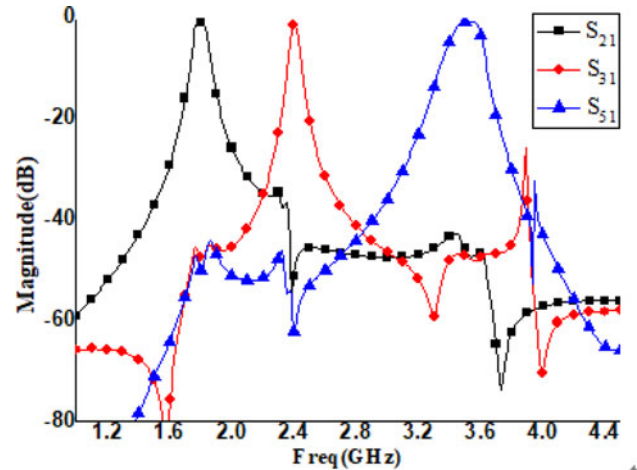
$$Z_{in} = jZ_2 \frac{2T - 0.5(\cot \theta_2 - \tan \theta_2)(\cot \theta_1 - \tan \theta_1)}{T(\cot \theta_2 - \tan \theta_2) + (\cot \theta_1 - \tan \theta_1)}, \quad (3)$$

where T is the impedance ratio, which is defined as $T = Z_2/Z_1$. The resonance occurs when $Z_{in} = \infty$, the resonant condition can be achieved:

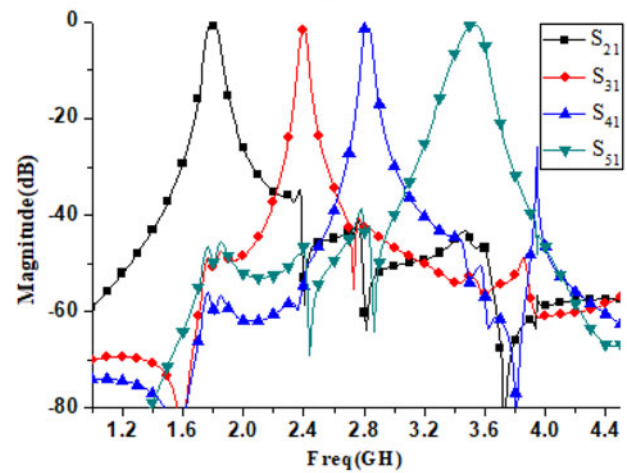
$$T(\cot \theta_2 - \tan \theta_2) + (\cot \theta_1 - \tan \theta_1) = 0. \quad (4)$$

Table 2. The final physical sizes of the presented quadplexer circuit (unit: mm)

W_0	W_1	W_2	W_3	W_4	l_0	l_1	l_2	l_3	W_{a1}
1.11	0.3	2.2	1.5	0.4	11	11.6	7	13.1	2.5
W_{a2}	l_{a1}	l_{a2}	g_a	t_a	W_{b1}	W_{b2}	l_{b1}	l_{b2}	g_{b1}
0.35	5.7	9.3	1.3	1.2	2	0.4	3	13	0.85
g_{b2}	t_b	W_{c1}	W_{c2}	W_{d1}	W_{d2}	l_{c1}	l_{c2}	l_{d1}	l_{d2}
0.4	0.2	1	0.38	1	0.4	7.6	16.6	6.4	14.2
g_{c1}	g_{c2}	g_{c3}	g_{d1}	g_{d2}	g_{d3}				
0.1	0.9	0.1	0.1	0.8	0.1				



(a)



(b)

Fig. 11. Transmission response. (a) Triplexer. (b) Quadplexer.

The length ratio β of the SIR is defined as $\beta = 2\theta_2/(\theta_1 + 2\theta_2) = 2\theta_2/\theta_t$. In the proposed circuit, the symmetrical SIRs are adopted, so the length ratio β is 0.5. The fundamental frequency f_0 is determined by the electrical lengths of the high-impedance and low-impedance line. In the proposed circuit, the electrical lengths of the high-impedance and low-impedance line θ_1 and θ_2 are both quarter-wavelength, which satisfies the resonant equation (4). Thus, the length of the open-loop SIR is half-wavelength. Figure 5(b) shows the coupling feed topology of the circuit, and

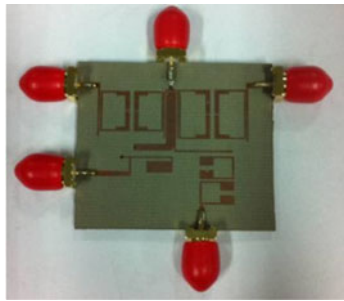
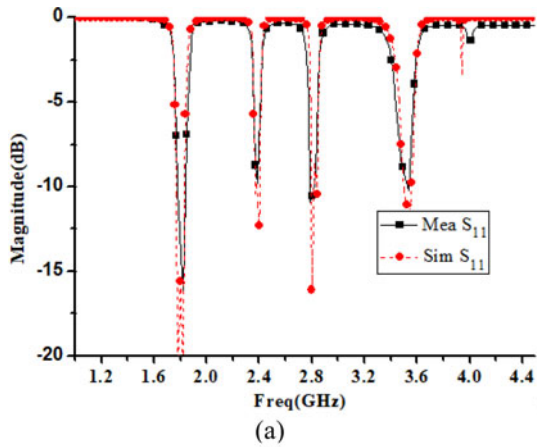
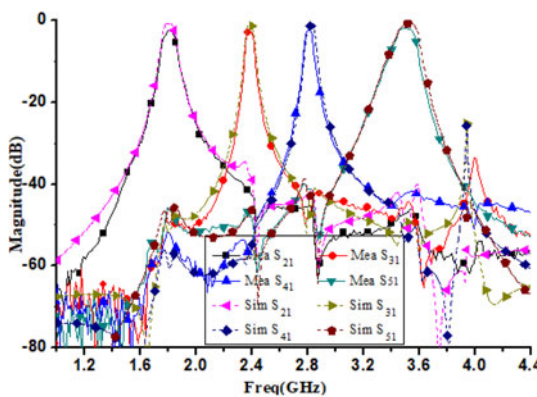


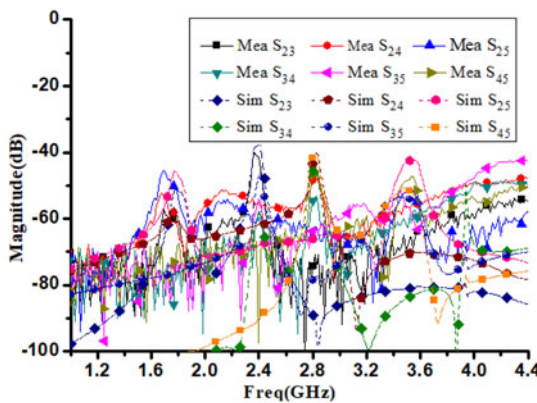
Fig. 12. Photograph of the fabricated quadplexer.



(a)



(b)



(c)

Fig. 13. Simulated and measured results. (a) Return loss. (b) Insertion loss. (c) Isolation.

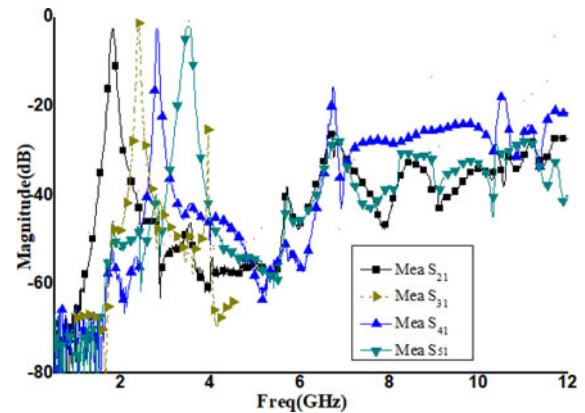


Fig. 14. Wideband response of the proposed quadplexer.

it is obvious that the external quality factor is related to the gaps S_1 and S_2 , and the desired return loss can be acquired by selecting appropriate gaps S_1 , S_2 and appropriate widths of the resonator.

The channels (port 2 and port 5) coupled with the short-circuit and open-circuit branches are realized by SIRs, and the central frequencies and relative bandwidths are 1.8/3.5 GHz and 5.1/5.7%, respectively. The shorted quarter-wavelength SIR and open-loop half-wavelength SIR are used for the first and the second passbands, respectively. Based on the circuit performance index above, the external quality factor Q_e and coupling coefficient K of each channel filter can be obtained by the synthesis method in the filter design software, and the external quality factor and coupling coefficient of the presented circuit are shown in Table 1. After that, the next step is to extract external quality factor and coupling coefficient of the simulated circuit model in HFSS, which can be used to determine the physical sizes of the filters.

Figure 6 shows the relationship between Q_e , l_0 , and g_0 , and the external quality factor Q_e of the common resonator is mainly related to the length of coupling line l_0 and the coupling slot g_0 . In addition, Q_{e0} and Q_{e1} are the first- and second-channel external quality factors, respectively. The coupling coefficients between shorted/open-loop SIRs and common resonator are shown in Fig. 7. It can be seen that the coupling coefficient is mainly related to the coupling gap (g_a and g_b). Through the extraction of the external quality factor and the coupling coefficient, the initial values of the corresponding parameters can be determined: $l_0 = 11$ mm, $g_0 = 0.15$ mm, $g_a = 0.95$ mm, $g_{b1} = 0.25$ mm, $g_{b2} = 0.4$ mm. Finally, by optimizing the sizes of the circuit based on the above initial values of the corresponding parameters, the transmission response of the channel 1 and channel 2 is given by Fig. 8, and it can be seen that the performance of the circuit meets the requirements, verifying the correctness of the design.

Based on the above circuit, the other two channels (port 3 and port 4) are added at the input feeder by the coupling feed technology, and the central frequencies and relative bandwidths are 2.4/2.8 GHz and 2.6/2.5%, respectively. The two open-loop half-wavelength SIRs are used for the third and the fourth passbands, respectively. The design procedure of the added channels is similar to that of the above circuit. Firstly, the external quality factor and coupling coefficient of each channel can be obtained by synthesis method, and the external quality factor and coupling coefficient of the presented circuit are shown in Table 1. Secondly, the

Table 3. The comparison with some prior works

Ref.	Return loss (dB)	Isolation (dB)	Central frequency (GHz)	Insertion loss (dB)	Out-of-band rejection (dB)	Relative bandwidth	Size ($\lambda g \times \lambda g$)
[9]	>10	>35	1.9/2.3/2.6	2.95/2.9/2.9	>35	12.2/4.25/7.3%	0.97×1.13
[10]	>15	>34	1.49/1.6/2.06/2.25	3.1/2.86/2.86/2.76	>30	6.3/6.45/6.34/6.6%	1.14×1.13
[11]	>10	>25	1.5/1.8/2.1/2.4	2.9/2.88/2.75/2.7	>35	3.5/3.5/4/4%	0.59×0.31
[12]	>11	>31	3.2/3.7/4.2/4.7	3.05/3.1/3.14/3.23	>35	3.4/2/2.5/2.5%	0.16×0.31
[13]	>15	>40	1.81/2.23/3.5/4.02	2.8/2.1/2.8/2.8	>40	7.8/9.1/5.7/5.0%	0.44×0.45
This work	>15	>40	1.8/2.4/2.8/3.5	2.4/2.6/2.8/2.5	>40	5.1/2.6/2.55/5.74%	0.36×0.42

initial values of the physical sizes can be obtained by extracting the external quality factor and coupling coefficient. Finally, the final physical sizes of the quadplexer can be determined by optimization.

The extracted external quality factors of the expanded channels are shown in Fig. 9, and Q_{e3} and Q_{e4} are the third- and fourth-channel external quality factors, respectively. Similarly, the coupling coefficients of the expanded channels are shown in Fig. 10, where K_3 is the coupling coefficient between channel 3 and the common resonator, and K_4 is the coupling coefficient between channel 4 and the common resonator. By extracting the external quality factor and the coupling coefficient, the initial values of the circuit can be determined: $gc_1 = gc_3 = 0.15$ mm, $gd_2 = 0.5$ mm, $gd_3 = 0.1$ mm, $gd_4 = 0.5$ mm.

Finally, the transmission response of the channel 3 and channel 4 is given by Fig. 11, and it can be seen that the two extra channels added at the input feeder have little effect on the existing channels. In other words, the implementation of the common input will not change the characteristics of the channel filters. In addition, the performance of the circuit meets the requirements, verifying the correctness of the design. Therefore, the quadplexer can be realized by adopting this structure.

Implementation and measurements

Through the above analyses, the compact high-isolation quadplexer is designed and fabricated with the substrate Taconic RF-35. The related parameters of this substrate are as follows: dielectric constant ϵ_r of 3.5, a thickness of 0.508 mm, and a loss tangent of 0.0018. The structure is simulated and optimized in Ansys-HFSS. Table 2 shows the final physical sizes of the presented quadplexer circuit. Figure 12 shows the fabricated miniaturized high-isolation quadplexer. The total size of the fabricated quadplexer is $0.36 \lambda g \times 0.42 \lambda g$. What's more, all the ports are connected by the type-SMA connectors.

The simulated and measured results of the proposed quadplexer are shown in Fig. 13. The measured central frequencies and 3 dB relative bandwidths of the quadplexer are 1.8/2.4/2.8/3.5 GHz and 5.1/2.6/2.55/5.74%, respectively. The measured return losses of four passbands are all greater than 12 dB, as shown in Fig. 13(a). Moreover, Fig. 13(b) shows that the measured insertion losses of the four passbands are 2.4/2.6/2.8/2.5 dB, respectively, including the losses of connectors and the error of the fabrication. The measured isolation of the entire frequency band is all greater than 40

dB, as shown in Fig. 13(c). Figure 14 shows the measured wideband response of the proposed quadplexer. It can be seen that the 20 dB upper stopband of the presented quadplexer is up to about 12 GHz. In addition, the measured results show a reasonable agreement with the simulated ones over the operating frequency range. Table 3 gives a comparison with some prior works. It can be seen that the proposed quadplexer has the advantages of compact size, wide out-of-band rejection, high isolation, low insertion loss, and good impedance matching.

Conclusion

A compact multimode-resonator quadplexer with wide upper-stopband and high isolation has been presented. The open and short stub-loaded multimode resonator and the curved SIRs are adopted in the quadplexer so as to reduce the size of the circuit. To analyze the proposed quadplexer, the equivalent topology circuit has been used. The measured results of the miniaturized high-isolation quadplexer agree well with the simulated ones. From the measured results, it can be seen that many advantages of the proposed quadplexer can be summarized as follows: compact size, superior isolation, wide upper-stopband, low insertion loss, and good impedance matching.

Acknowledgement. The work was supported in part by the National Natural Science Foundation of China (Grant No: 61771094) and by Sichuan Science and Technology Program (Grant No: 2019JDR0008).

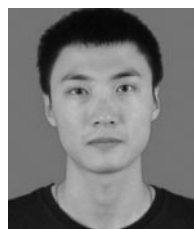
References

- Chen CJ (2018) A coupled-line coupling structure for the design of quasi-elliptic bandpass filters. *Microwave Theory and Techniques, IEEE Transactions on* **66**, 1921–1925.
- Liu H, Xu W and Zhang Z (2013) Compact diplexer using slotline stepped impedance resonator. *IEEE Microwave and Wireless Components Letters* **2**, 75–77.
- Tanii K and Wada K (2013) Frequency diplexer using multimode bandpass filters with high stopband attenuation level. *Electronics Letters* **16**, 1011–1013.
- Tu WH, Hung WC and Du TH (2015) Design of microwave microstrip multiband diplexers for system in package. *IEEE Transactions on Components, Packaging, Manufacturing Technology* **4**, 502–507.
- Peng HS and Chiang YC (2015) Microstrip diplexer constructed with new types of dual-mode ring filters. *IEEE Microwave & Wireless Components Letters* **25**, 7–9.

6. **Huang Y, Wen G and Li J** (2014) Compact microstrip triplexer based on twist-modified asymmetric split-ring resonators. *Electronics Letters* **23**, 1712–1713.
7. **Song K, Zhou YD, Chen YX, Patience SR, Guo S and Fan Y** (2019) Compact high-isolation multiplexer with wide stopband using spiral defected ground resonator. *IEEE Access* **7**, 31702–31710.
8. **Yassini B and Yu M** (2015) Ka-Band dual-mode super Q filters and multiplexers. *IEEE Transactions on Microwave Theory and Techniques* **63**, 3391–3397.
9. **Taravati S and Amirhosseini MK** (2013) Design method for matching circuits of general multiplexers. *IET Microwaves, Antennas & Propagation* **7**, 237–244.
10. **Deng PH, Huang BL and Chen BL** (2015) Designs of microstrip four and five-channel multiplexers using branch-line-shaped matching circuits. *IEEE Transactions on Components, Packaging and Manufacturing Technology* **5**, 1331–1338.
11. **Hung WC, Hsu KW and Tu WH** (2013) Wide-stopband microstrip quadruplexer using asymmetric stepped-impedance resonators. *IEEE MTT-S International Microwave Symposium Digest*, Seattle, WA, USA, pp. 1–4.
12. **Lo SS, Hsu KW and Tu WH** (2013) Compact and high-isolation microstrip quadruplexer. *Proceedings of Asia-Pacific Microwave Conference*, Seoul, South Korea, pp. 966–968.
13. **Shao Q and Chen FC** (2017) Design of compact and high-isolation quadruplexer with novel matching network. *IEEE Access* **5**, 11374–11380.
14. **Zhao P and Wu KL** (2014) An iterative and analytical approach to optimal synthesis of a multiplexer with a star-junction. *IEEE Transactions on Microwave Theory and Techniques* **62**, 3362–3369.
15. **Duan Q, Song K, Zhu Y, Fan M, Chen F and Li L** (2015) Compact wide-stopband diplexer using dual mode resonators. *Electronics Letters* **51**, 1085–1087.
16. **Hu H, Wu KL and Cameron RJ** (2013) Stepped circular waveguide dual-mode filters for broadband contiguous multiplexers. *IEEE Transactions on Microwave Theory and Techniques* **61**, 139–145.
17. **Hong S and Chang K** (2010) A 10–35-GHz six-channel microstrip multiplexer for wide-band communication systems. *IEEE Transactions on Microwave Theory and Techniques* **54**, 1370–1378.
18. **Bukuru D, Song K and Ren X** (2015) Compact wide-stopband planar diplexer based on rectangular dual spiral resonator. *Microwave and Optical Technology Letters* **57**, 174–178.
19. **Lin SC and Yeh CY** (2015) Design of microstrip triplexer with high isolation based on parallel coupled-line filters using T-shaped short-circuited resonators. *IEEE Microwave and Wireless Components Letters* **25**, 648–650.
20. **Zeng SJ, Wu JY and Tu WH** (2011) Compact and high-isolation quadruplexer using distributed coupling technique. *IEEE Microwave and Wireless Components Letters* **21**, 197–199.
21. **Chi PL and Yang T** (2016) Novel 1.5–2.4 GHz tunable single-to-balanced diplexer. *IEEE Microwave and Wireless Components Letters* **26**, 783–785.
22. **Snyder RV, Mortazawi A and Hunter I** (2015) Present and future trends in filters and multiplexers. *IEEE Transactions on Microwave Theory and Techniques* **63**, 3324–3360.
23. **Xu J** (2016) Compact switchable bandpass filter and its application to switchable diplexer design. *IEEE Microwave and Wireless Components Letters* **26**, 13–15.
24. **Kurra L, Abegaonkar MP and Basu A** (2014) A harmonic suppressed bandpass filter and its application in diplexer. *IEEE Microwave and Wireless Components Letters* **24**, 388–390.
25. **Zhou Y, Deng HW and Zhao Y** (2014) Compact balanced-to-balanced microstrip diplexer with high isolation and common-mode suppression. *IEEE Microwave and Wireless Components Letters* **24**, 143–145.
26. **Cheng F, Lin X and Song K** (2013) Compact diplexer with high isolation using the dual-mode substrate integrated waveguide resonator. *IEEE Microwave and Wireless Components Letters* **23**, 459–461.
27. **Deng PH and Tsai JT** (2013) Design of microstrip lowpass-bandpass diplexer. *IEEE Microwave and Wireless Components Letters* **23**, 332–334.



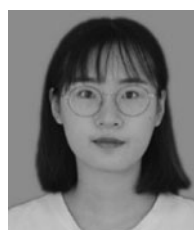
Kaijun Song received the M.S. degree in radiophysics and the Ph.D. degree in electromagnetic field and microwave technology from the University of Electronic Science and Technology of China (UESTC), Chengdu, China, in 2005 and 2007, respectively. In 2011, he received the “New Century Excellent Talents in University Award” from the Chinese Ministry of Education. In 2015, he received the academic and technical leaders in Sichuan province. Since 2007, he has been with the EHF Key Laboratory of Science, School of Electronic Engineering, UESTC, where he was a Full Professor. From 2018, he is currently a Full Professor with the School of Electronic Science and Engineering, UESTC. From 2007 to 2008, he was a post-doctoral research fellow with the Montana Tech of the University of Montana, Butte, USA, working on microwave/millimeter-wave circuits and microwave remote-sensing technologies. From 2008 to 2010, he was a research fellow with the State Key Laboratory of Millimeter Waves of China, Department of Electronic Engineering, City University of Hong Kong, on microwave/millimeter-wave power-combining technology and Ultra-Wideband (UWB) circuits. He was a senior visiting scholar with the State Key Laboratory of Millimeter Waves of China, Department of Electronic Engineering, City University of Hong Kong in November 2012. He has published more than 200 internationally refereed journal papers and conference papers. His current research fields include microwave and millimeter-wave/THz power-combining technologies; high-power solid-state microwave/millimeter-wave technologies; UWB circuits and technologies; and microwave/millimeter-wave devices, circuits, and systems. Prof. Song is the Reviewer of tens of international journals, including IEEE Transactions and IEEE Letters.



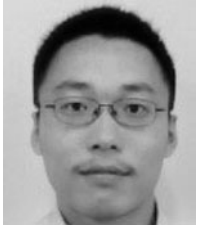
Mou Luo was born in Sui Ning, Sichuan Province, China, in September 1996. He received the B.Sc. degree in Engineering from Southwest Jiaotong University, Chengdu, China, in 2018, and is currently working toward the Master's degree in electronic science and technology at the University of Electronic Science and Technology of China. His research interests include microwave/millimeter-wave circuits and systems and Terahertz wave power-combining technologies.



Cuilin Zhong was born in Hengyang, Hunan, China. He received the M.Sc. degree and D.Sc. degree, respectively, in 2004 and 2009 with major at radio physics from the University of Electronic Science and Technology of China (UESTC), Chengdu, China. From August 2004 to November 2006, he worked on the RF technology research and development of wireless and mobile communication, and he is the team leader of the Department of Microwave Circuit MCM in GUOREN communication company. His research interests include the microwave, antenna techniques, and radio technology of wireless communication and radar.



Yuxuan Chen was born in Nan Chang, Jiangxi Province, China, in April 1996. She received the B.Sc. degree in Engineering from Southwest University, Chongqing, China, in 2018, and is currently working toward the Ph.D. degree in electronics and communication engineering at the University of Electronic Science and Technology of China. Her research interests include microwave/millimeter-wave and Terahertz wave power-combining technologies.



Yedi Zhou was born in Harbin, Heilongjiang Province, China, in January 1991. He received the B.S. degree from the University of Electronic Science and Technology of China (UESTC), Chengdu, China, in 2013. He is currently pursuing the Ph.D. degree in electromagnetic fields and microwave technology at UESTC. His research interests include microwave and millimeter-wave power-combining

technology.



Fei Xia was born in Sichuan, China, in 1994. He received the B.S. degree from Xidian University of Electronic Technology, Xian, China, in 2017. He is currently working toward the M.S. degree in the School of Electronic Science and Technology of China, Chengdu, China. He is interested in microwave technologies.